

Supporting information for

## ***In-situ* Growth of $\alpha$ -CsPbI<sub>3</sub> Perovskite Nanocrystals on the Surface of Reduced Graphene Oxide with Enhanced Stability and Carrier Transport Quality**

*Qi Zhang<sup>1</sup>, Hui Nan<sup>1</sup>, Yangying Zhou<sup>1</sup>, Youchen Gu<sup>1</sup>, Meiqian Tai<sup>1</sup>, Yaxuan Wei<sup>1</sup>, Feng Hao<sup>2\*</sup>,*

*Jianbao Li<sup>3,1</sup>, Dan Oron<sup>4,\*</sup> and Hong Lin<sup>1,\*</sup>*

<sup>1</sup> State Key Laboratory of New Ceramics & Fine Processing, School of Materials Science and Engineering, Tsinghua University, Beijing 100084, China

<sup>2</sup> School of Materials and Energy, University of Electronic Science and Technology of China, Chengdu 610054, China

<sup>3</sup> State Key Laboratory of Marine Resource Utilization in South China Sea, Materials and Chemical Engineering Institute, Hainan University, Haikou 570228, China

<sup>4</sup> Department of Physics of Complex Systems, Weizmann Institute of Science, Rehovot 76100, Israel

**Table S1.** Structural parameters derived from the corresponding XRD patterns of  $\alpha$ -CsPbI<sub>3</sub> NCs and  $\alpha$ -CsPbI<sub>3</sub> NCs/rGO heterostructures. The crystal sizes of  $\alpha$ -CsPbI<sub>3</sub> NCs are calculated by Debye-Scherrer equation. (Instrument correction value for instrumental broadening changes =0.1252 °)

	Full width at half maximum of (200) Peak, °	Calculated crystal size, nm
$\alpha$ -CsPbI <sub>3</sub> NCs	0.87	10.64
$\alpha$ -CsPbI <sub>3</sub> NCs/rGO	0.79	11.83

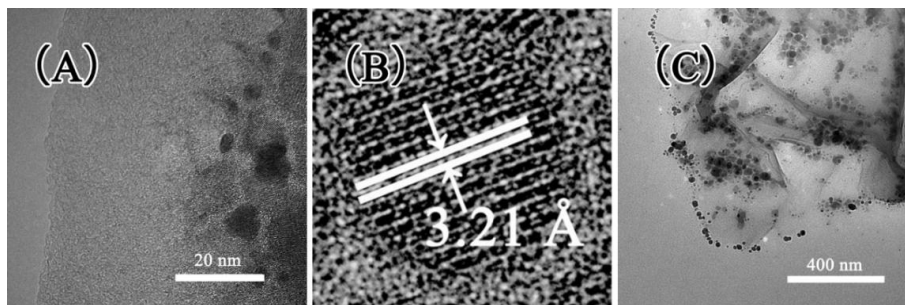


**Figure S1.** (A) TEM image of  $\alpha$ -CsPbI<sub>3</sub> NCs/rGO heterostructures with a few Pb-nanoparticles appeared on the surface of rGO. (B) HRTEM image of  $\alpha$ -CsPbI<sub>3</sub> NCs. The lattice figure of these NCs shows a value of  $\sim 3.21$  Å, which is consistent with the crystal structure of  $\alpha$ -CsPbI<sub>3</sub> perovskite. (C) TEM image of  $\alpha$ -CsPbI<sub>3</sub> NCs/rGO heterostructures, and rGO was reduced by thermal-reduced reaction without FeI<sub>2</sub> treatment. Thus  $\alpha$ -CsPbI<sub>3</sub> NCs showed a stochastic distribution on the surface of rGO and their shapes were not regular.

**Table S2.** Element contents derived from the corresponding XPS spectra of  $\alpha$ -CsPbI<sub>3</sub> NCs and  $\alpha$ -CsPbI<sub>3</sub> NCs/rGO. The element contents are normalized to investigate the effect of *in-situ* growth method on ligands amounts on the surface of  $\alpha$ -CsPbI<sub>3</sub> NCs (Pb contents can be regarded as 1). It is clear that the amount of  $\alpha$ -CsPbI<sub>3</sub> NCs obviously increased and the amount of C and O elements related to ligands significant decrease.

	$\alpha$ -CsPbI <sub>3</sub> NCs	$\alpha$ -CsPbI <sub>3</sub> NCs/rGO
Pb 4f	1.00	1.00
C 1s	63.11	17.37
N 1s	2.00	0.73
O 1s	25.04	1.71
I 3d	4.01	4.34
Cs 3d	1.00	1.23

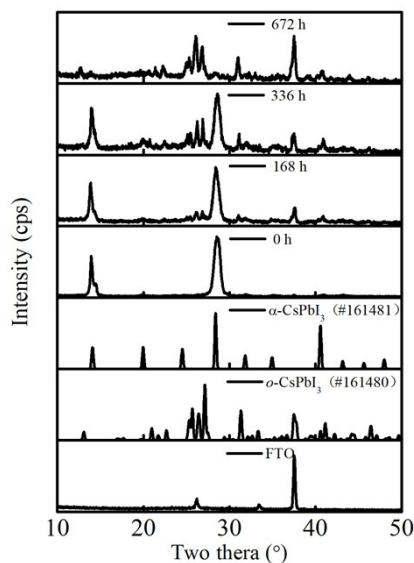


**Figure S2.** XRD patterns of  $\alpha$ -CsPbI<sub>3</sub> NCs as a function of storage times stored in dark, low temperature ( $\sim 4$  °C) and low humidity ( $\sim 1\%$  RH) conditions without encapsulation. The recording storage times were  $\sim 0$  h,  $\sim 168$  h,  $\sim 336$  h and  $\sim 672$  h. The standard XRD patterns of FTO, *o*-CsPbI<sub>3</sub> (#161480) and  $\alpha$ -CsPbI<sub>3</sub> (#161481) are also listed to identify the structural transitions of as-synthesized  $\alpha$ -CsPbI<sub>3</sub> NCs. These XRD patterns showed that the  $\alpha$ -CsPbI<sub>3</sub> NCs can easily transform into *o*-CsPbI<sub>3</sub> even when stored in dark, low temperature ( $\sim 4$  °C) and low humidity ( $\sim 1\%$  RH) conditions without encapsulation, completely losing their ideal crystal structure of optically active materials.

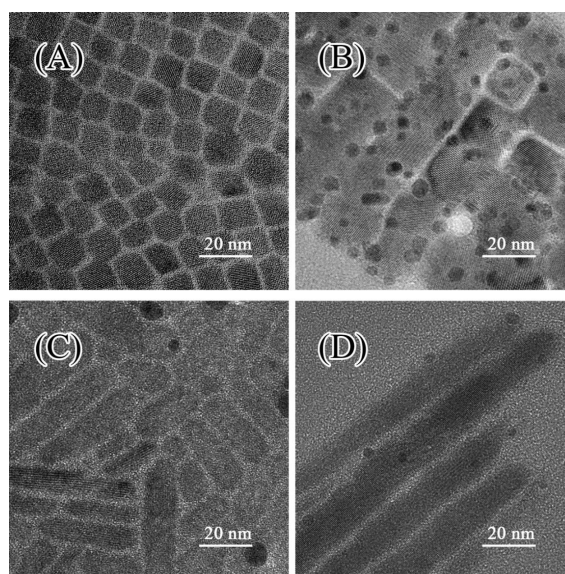


**Figure S3.** TEM images of  $\alpha$ -CsPbI<sub>3</sub> NCs as a function of storage times stored in dark, low

temperature ( $\sim 4\text{ }^{\circ}\text{C}$ ) and low humidity ( $\sim 1\%$  RH) conditions without encapsulation. The recording storage times were (A)  $\sim 0$  h, (B)  $\sim 168$  h, (C)  $\sim 336$  h and (D)  $\sim 672$  h.

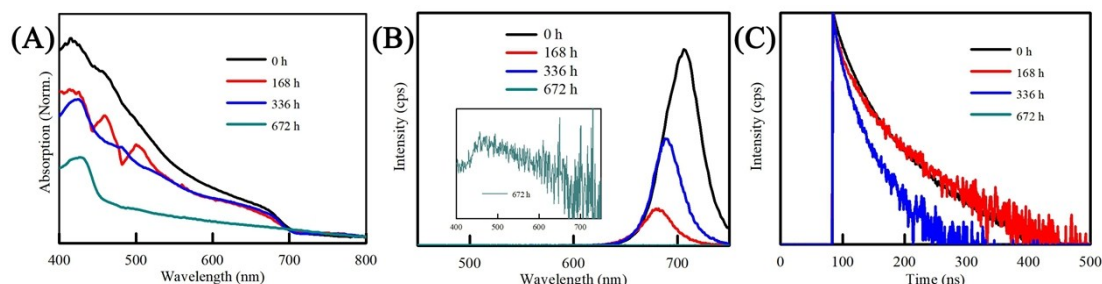


**Figure S4.** (A) UV-Visible absorption, (B) steady-state PL, and (C) time-resolved PL spectra of  $\alpha$ -CsPbI<sub>3</sub> NCs as a function of storage times stored in dark, low temperature ( $\sim 4\text{ }^{\circ}\text{C}$ ) and low humidity ( $\sim 1\%$  RH) conditions without encapsulation. The recording storage times were  $\sim 0$  h,  $\sim 168$  h,  $\sim 336$  h and  $\sim 672$  h. These UV-Visible absorption spectra showed a significant blue-shift of the absorption peaks when the storage time increased, thus narrowing their coverage of the visible region. Meanwhile, when the storage time increased, these PL intensities decreased and the PL bands showed a blue-shift, and their lifetime of  $\alpha$ -CsPbI<sub>3</sub> NCs reduced. Particularly, when the storage time approaches  $\sim 672$  h, the band gap of  $\alpha$ -CsPbI<sub>3</sub> showed a value of  $\sim 2.64$  eV, and the intensity of CsPbI<sub>3</sub> NCs almost disappeared, and their lifetime were hardly to detect in the testing conditions, completely losing their optoelectronic properties of optically active materials.

**Table S3.** Peak positions and Lifetime derived from the corresponding steady-state PL and time-resolved PL spectra of  $\alpha$ -CsPbI<sub>3</sub> NCs as a function of storage times stored in dark, low temperature ( $\sim 4\text{ }^{\circ}\text{C}$ ) and low humidity ( $\sim 1\%$  RH) conditions without encapsulation.

	Steady-state PL		Time-resolved PL		
	Peak position, nm	$\tau_1$ , ns	$\tau_2$ , ns	$\tau_3$ , ns	$\tau_{\text{aver}}$ , ns
0h	706.00	10.09	29.59	104.92	32.10
168h	688.00	7.49	29.40	97.74	25.45
336h	680.00	2.01	14.01	51.63	10.57
672h	-	-	-	-	-

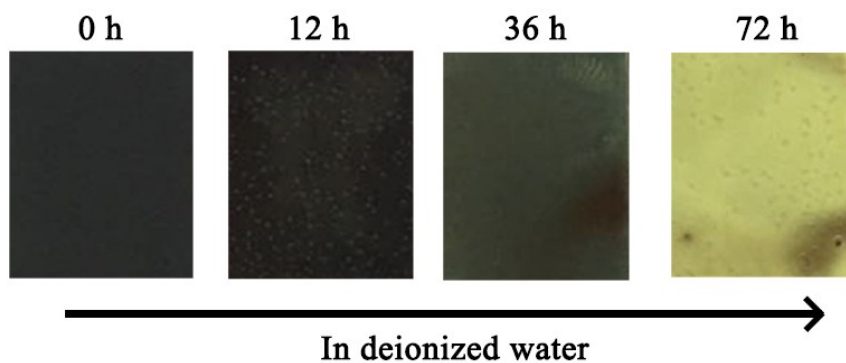


**Figure S5.** The color of  $\alpha$ -CsPbI<sub>3</sub> NCs as a function of storage times placed in deionized water without encapsulation.

**Table S4.** Optoelectronic parameters derived from corresponding UV-Visible absorption, steady-state PL and time-resolved PL spectra of  $\alpha$ -CsPbI<sub>3</sub> NCs and  $\alpha$ -CsPbI<sub>3</sub> NCs/rGO heterostructures films.

	UV-Visible	Steady-state PL	Time-resolved PL			
	Band gap, eV	Peak Position, nm	$\tau_1$ , ns	$\tau_2$ , ns	$\tau_3$ , ns	$\tau_{aver}$ , ns
$\alpha$ -CsPbI <sub>3</sub> NCs	1.72	706.00	10.09	29.59	104.92	32.10
$\alpha$ -CsPbI <sub>3</sub> NCs/rGO	1.74	688.00	12.29	45.28	125.48	67.77

**Table S5.** Structural parameters and Lifetime derived from the corresponding XRD patterns and time-resolved PL spectra of  $\alpha$ -CsPbI<sub>3</sub> NCs and  $\alpha$ -CsPbI<sub>3</sub> NCs/rGO stored in ambient conditions (room temperature of  $\sim 25$  °C and a humidity of  $\sim 25\%$  RH conditions) for  $\sim 4$  weeks without encapsulation. (Instrument correction value for instrumental broadening changes = 0.1252 °)

	XRD		Time-resolved PL			
	Full width at half maximum of (200) Peak, °	Calculated crystal size, nm	$\tau_1$ , ns	$\tau_2$ , ns	$\tau_3$ , ns	$\tau_{aver}$ , ns
$\alpha$ -CsPbI <sub>3</sub> NCs	-	-	-	-	-	-
$\alpha$ -CsPbI <sub>3</sub> NCs/0.2-rGO	0.74	12.83	10.93	39.01	111.17	49.39

**Table S6.** PLQYs of  $\alpha$ -CsPbI<sub>3</sub> NCs and  $\alpha$ -CsPbI<sub>3</sub> NCs/rGO heterostructures films stored in ambient conditions for ~4 weeks without encapsulation.

	0 weeks, %	1 weeks, %	2 weeks, %	3 weeks, %	4 weeks, %
$\alpha$ -CsPbI <sub>3</sub> NCs	11.22	6.11	3.53	0.86	0.18
$\alpha$ -CsPbI <sub>3</sub> NCs/rGO	10.74	10.22	9.43	8.34	7.28